

COMPARITIVE SCALED MMLS3 TESTS VS. FULL-SCALE MLS10 TESTS IN MOZAMBIQUE

AUGUST 2006

By

Eben R. de Vos
Researcher : Institute for Transport Technology
Department of Civil Engineering
University of Stellenbosch
Private Bag X1
STELLENBOSCH
South Africa
7600
Tel. +27 (0)21 808-4079
Fax.+27 (0)21 808-4361
Email: erdevos@sun.ac.za

Pieter Strauss
Consultant
P O BOX 588
LA MONTAGNE
0184
tel & fax : 012 807 0367
E-Mail: pieterst@lantic.net

Kenneth W. Fults
Senior Research Fellow
Center for Transportation Research, Suite 200
College of Engineering Research
University of Texas at Austin
3208 Red River
Austin, TX 78705-2650
Phone: (512) 232 -3081
Fax: (512) 232 -3070
E-mail: kenfults@yahoo.com

Fred Hugo
Director: Institute for Transport Technology
Department of Civil Engineering
University of Stellenbosch
Private Bag X1
STELLENBOSCH
South Africa
7600
Tel. +27 (0)21 808-4364
Fax.+27 (0)21 808-4361
Email: fhugo@sun.ac.za

Jorge A. Prozzi
The University of Texas
Department of Civil Engineering
1 University Station, #C1761
ECJ Bldg., Suite 6.112
Austin, TX 78712-0278
Phone: (512) 232-3488
Fax: (512) 475-8744
Email : prozzi@mail.utexas.edu

Hilário Tayob
ANE Project coordinator
National Administration of roads
Directorate of National Roads
Engineering Department
Av. de Moçambique 1225, C.P. 1439
Maputo - Mozambique
Phones +25821476163/7 - Fax +25821475862
Email : htayob@ane.gov.mz

Abstract

Mozambique is rehabilitating and upgrading its roadway infrastructure. It found some consulting engineers and contractors were not familiar with Mozambique conditions and materials. The World Bank sponsored a research project to support these preservation and maintenance efforts. The object is to develop guidelines for a mechanistic-empirical pavement design method for cement stabilized sand bases in Mozambique based on *Accelerated Pavement Testing (APT)* technology. The APT encompasses both scaled (one third) and full-scale APT using mobile load simulator technology (MMLS3 and MLS10)

MMLS3 testing was used to scope research and provide guidelines for the selection and construction of full-scale test sections on natural subgrade. MLS10 expanded the investigation through testing of the full-scale pavements, including wet trafficking cycles to emulate environmental effects.

Initial findings show good comparative compatible tests results of scaled and full-scale pavements in terms of trends in stiffness change as measured with the P SPA, distress mechanisms and surface deformation relative to respective wheel loads and number of load applications. Manifested distress mechanisms under APT were also similar to those found in pavement structures in the region.

MLS10 is operational since April 2006. Four sets of dual wheels each loaded to 60kN run in a closed loop with a maximum speed of up to 26kph. Operation is similar to the MMLS3. The latter was has four single tyres each carrying 2.7 kN. Ten MMLS3 tests including two field tests have been completed as well as three MLS10 tests.

Keywords

Accelerated Pavement Testing, cement-treated bases, sand bases, mechanistic design, compatibility of findings, stiffness, distress mechanisms

No. of Words

7483

INTRODUCTION

Mozambique is investing heavily in rehabilitating and upgrading its roadway infrastructure. Extensive use has been made of consulting engineers and contractors some of whom were not necessarily familiar with Mozambique conditions and materials. The World Bank sponsored a research project to support these preservation and maintenance efforts. The object is to develop guidelines for a mechanistic-empirical pavement design method for cement stabilized sand bases in Mozambique based on *Accelerated Pavement Testing (APT)* technology. The APT program encompasses both scaled (one third) and full-scale APT using mobile load simulator technology (MMLS3 and MLS10). Table 1 shows a comparison between MMLS3 and MLS10 APT machine test parameters (Strauss et al, 2005).

TABLE 1 Comparison of MMLS3 and MLS10 APT Machine Parameters

	Item		1/3 Scale MMLS3	Standard MLS10
1	Testing length	m	1	4
2	Tread path width	mm	80	610
3	Size of test section	m	1 x 0.4 (min)	5 x 1.6
4	Wheel configuration		Single	Dual
5	No of wheels		4	4
6	Trolley description		Four bogies with spring suspension	Four bogies with pneumatic hydraulic suspension
7	Wheel load	kN	2.7	60
8	Wheel velocity	m/s	2.5	7.2
9	Repetition /h		7200	7200
10	Tyres		Vredestein 6 ply pneumatic	Continental R22.5 295/65
11	Tyre pressure	kPa	700	800
12	Trafficking conditions		Dry, heated, wet heated	Dry, Wet

The research reported in this paper forms part of a program that was developed through a workshop that involved all affected parties. The scope of the paper is limited to a presentation of the comparative findings with the MMLS3 and the MLS10 APT trafficking in terms of distress and performance. The validity of scaled pavement testing was investigated in detail by Kim et al (1998) .

The APT section of the project is focused on three primary aspects:

- Exploratory scaled laboratory MMLS3 testing
- Construction of field test sections
- Full-scale and scaled field APT by means of MLS10 and MMLS3

The purpose of using the MMLS3 was to evaluate the performance of the stabilized coastal sands under different trafficking conditions in the laboratory. This was to be the basis for identifying potential failure mechanisms for comparison with failure mechanisms observed in the field. Table 2 depicts the full MMLS3 test matrix that is being undertaken. In similar vein, this information was used to provide the basis for formulation of the specifications for constructing full scale test sections to be tested by the MMLS3 and the MLS10. It is also being used as input for the mechanistic modelling that is being developed. Ten MMLS3 tests, including two field tests have been completed as well as three MLS10 tests.

The field APT trials are being executed to cover the optimum number of test sections. The selection was to be based on a progressive review of the findings. Accordingly decisions on the number of load applications and degree of distress of the respective test sections would not be fixed beforehand. Diagnostic evaluation would form an integral part of the selection.



FIGURE 1 View of the MLS10 on the test site at Manhiça in Mozambique during trafficking

TABLE 2 Overview of the test matrix for the MMLS3 test program

Sand type	Base thickness, mm	Binder %	CEM32.5 II:Lime		Surfacing		Conditions	No of Tests
Palmeira Red	50	5	100:0	50:50		AC	◆20/50 °C Wet/Dry	2
Palmeira Red	50	7	100:0	50:50	Seal	AC	◆20/50 °C Wet/Dry	3
Palmeira Red	50	3	100:0		Seal	AC	◆20/50 °C Wet/Dry	2
Palmeira Red	150 (F)	5	100:0		<u>Seal</u> ⁺		* ◆20/50 °C Wet/Dry	1
Palmeira Red	150 (F)	5	ETB + CEM	ETB	Seal		*◆50 °C Dry	4
Palmeira Yellow	50	7	100:0		Seal ⁺	AC	◆20/50 °C Wet/Dry	2
Cores Red	100	5	100:0		Seal		◆20/50 °C Wet/Dry	1
* 50°C dry only ◆ 20/50°C equals wet temperature vs. heated trafficking temperature (F) equals MMLS3 Field tests ETB – Emulsion Treated Base , SS60 Emulsion was used - Beyond the scope of this paper								

EXPLORATORY SCALED LABORATORY TESTING PROGRAM

The MMLS3 testing matrix was established through an interactive workshop of all affected parties. Iterative reviews of the findings in terms of modes of failure, material response and performance under traffic loading were executed. The process included careful determination of failure mechanisms and comparison with observed performance of Mozambiquen highways.

Third scale pavements comprising a 50 mm stabilized base on top of a free draining sand subgrade, surfaced with a 20 mm HMA or double seal were constructed in the Stellenbosch laboratory. Pavements were constructed in metal boxes (1.2m x 3m) to eliminate edge effects on the trafficked width. Two base material types are being tested, these are respectively red and yellow colourish sand material available from the borrow-pits in the vicinity of the full-scale APT test site. These materials were used for rehabilitation of Highway EN1 and are representative of the coastal sands commonly found in Mozambique. The red sand has been found to perform better than the yellow sand. Laboratory tests have been used to determine the respective characteristics. Ordinary Portland Cement, CEM32.5 II, is being used as stabilizing agents at 3, 5 and 7 percent contents. Lime is blended with cement, 50:50, for selected tests.

It should be noted that the HMA was similar to that used for the construction of the test section and the adjacent pavement of highway EN1 except that the maximum particle size was reduced to 13 mm instead of 19 mm. The oversize particles were scalped off. In essence the mix thus comprised 40/50 penetration bitumen with a continuously graded 13 mm aggregate. Optimum binder content was selected on the basis of 7 % voids using gyratory compaction. The 13 mm chip seal was constructed as a double seal (9/6) using aggregate from the site and 60 percent stable grade emulsion supplied by Colas South Africa. Construction was performed using a chip spreader and spray bar specially developed for MMLS3 test bed. The binder application was enriched to enhance water tightness. In all cases the modified MC70 prime coat was the same as used on site. Both surfacing comprise local Mozambican materials based on proven design recipes.

Trafficking was conducted with the MMLS3 load characteristics as in Table 1. Environmental conditioning of the laboratory tests comprises cyclic dry heated and wet ambient pavement conditions. This is done to simulate critical field conditions. Trafficking was alternated between the heated mode of 200 000 load applications and the wet mode of 50 000 load applications. For the wet mode water at 20 °C is sprayed onto the pavement to simulate the flow of a 1 mm thick sheet of water across the surface during trafficking. For the heated dry mode hot air is blown across the pavement surface to maintain a surface temperature of 55 °C.

Stiffness and rutting was monitored using the Portable Seismic Pavement Analyser (PSPA) and a profilometer respectively. The Portable Seismic Pavement Analyzer (PSPA) is used to determine the average modulus of a pavement layer (Nazarian et al, 2002,) (Nazarian et al 1997). The operating principle of the PSPA is based on generating and detecting stress waves in a medium. The Ultrasonic Surface Wave (USW) method, which is an offshoot of the SASW method, can be used to determine the modulus of the material. The theoretical and experimental background behind this method can be found in Baker et al. (1995). A seismic source and at least two receivers are needed. The source impacts the surface of the medium to be tested and the transmitted waves are monitored with the receivers. By conducting a spectral analysis, a so-called dispersion curve (a plot of velocity of propagation of surface waves with wavelength) is obtained. The average modulus of the top layer, E_{USW} , can be obtained from the average phase velocity, V_{ph} :

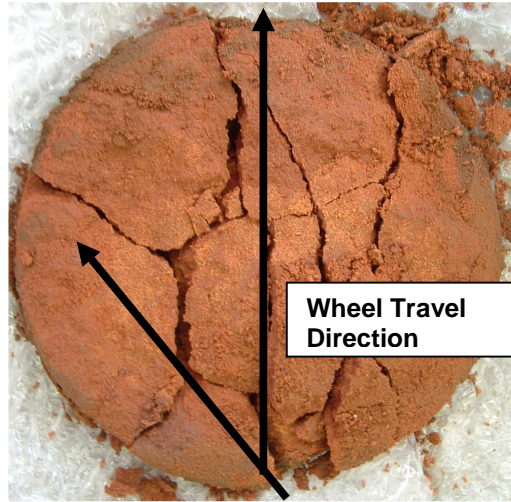
$$E_{USW} = 2\rho(1+\nu)[(1.13-0.16\nu)V_{ph}]^2 \quad [1]$$

Where ρ is the mass density in kilograms per square meter and ν is the Poisson's Ratio. Ratios of trafficked stiffness to original stiffness were used as the basis of evaluation of the distress that had set in under trafficking. Seismic stiffness ratios were intermittently measured in two directions, longitudinal and transverse, relative to the wheel path. This was done to evaluate the development of pavement failure in two perpendicular directions and relate the decreasing stiffness ratio's with different failure mechanisms once diagnostic investigation are done after traffic completion.

Performance Evaluation of Scaled APT by means of MMLS3

Under MMLS3 laboratory trafficking the red coastal sand performed well after stabilizing with cement or a lime cement blend. The sections with higher cementations binders performed better. The seven percent sections withstood trafficking in excess of three million axle load applications. The five and three percent sections carried in excess of one million and 150 00 axle load applications respectively.

1
2
3 Figures 2 and 3 depict images taken after the diagnostic analyses of the test pavements. Such
4 diagnostic views are of great help in determining the nature of the distress in a pavement system. Details
5 pertaining to the respective tests can be found in Table 3.



19 **FIGURE 2** Top view of lower half of red sand 3 % CTB layer exhibiting shear failure, failure planes
20 parallel to direction of travel on edges of wheel track.



40 **FIGURE 3a** Side view of beams taken from 3 percent cement section. Note different phases of failure.

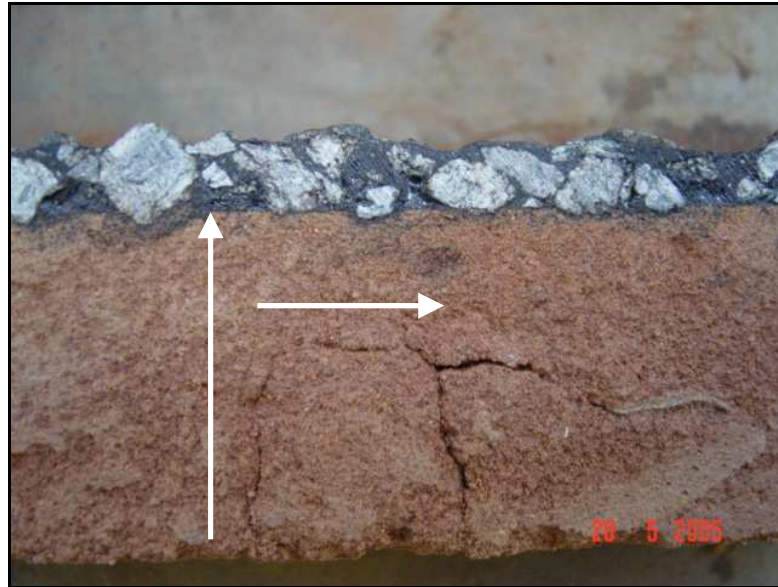


FIGURE 3b Close up of 3 percent cement beam with seal, extracted from the scaled laboratory pavement, shear plane on neutral axis clearly visible (50 mm high, length of shear plane 20 mm)

Distress development in the high-strength cemented bases appears to differ from normal distress development in full depth AC pavements (Hugo et al, 2004) (Lee Sugjoon and Kim Richard, 2004). Micro fracturing that was detected relatively early did not seriously affect the stiffness of the pavement system.

The higher cement content bases did not manifest surface distress although the base had transverse and longitudinal cracks. To initiate a more typical mode of field and laboratory distress due to shrinkage cracks, transverse cracks were artificially created by drilling small holes through the pavement structure at 10 mm centres. Initially the holes were drilled 5mm deep with the intent of weakening the structure sufficiently to cause rupturing to follow throughout the structure. This did not occur and hence the holes were drilled to a depth of 25 mm and then through the full depth of the CTB.

It was not surprising to find that the performance extended well into several million load applications before distress manifested in the form of pumping at the point of artificial water ingress.

The CTB performed very well for a long time without distress setting in. The HMA did exhibit initial distress through rutting. This was traced to insufficient initial compaction (voids were nominally 13 % - the rutting was adjusted for initial traffic compaction). The result of this was an increase in the stiffness of the HMA as trafficking progressed. Only thereafter did the stiffness start reducing gradually until failure occurred in proximity of the artificial transverse crack. The performance of the 7 percent pavements was as expected, very good. Low rates of stiffness loss for the higher binder contents are evident.

1
2
3
4
5
6
7
8
9
10
11
12
13
14
15
16
17
18
19
20
21
22
23
24
25
26
27
28
29
30
31
32
33
34
35
36
37
38
39
40
41
42
43
44
45
46
47
48
49
50
51
52

TABLE 3 MMLS3 Test Results with Scaled Laboratory and Field Trafficking

MATERIAL SOURCE	STABILISING AGENT	SURFACING	AXLES TO FAILURE	DISTRESS MECHANISMS
PALMEIRA - RED	3 % CEM II 32.5	HMA	150 000	·Pumping of crushed material ·Horizontal and vertical shear ·Flexural cracking ·Interface distress
PALMEIRA - RED	3 % CEM II 32.5	SEAL	145 000	·Shear followed by bottom-up cracking up to neutral axis
PALMEIRA - RED	7 % CEM II 32.5 + 1.5 % LIME (ILC)	HMA	3 100 000	·Local distress induced by artificial transverse cracking ·Longitudinal flexural cracks (longitudinal growth)
PALMEIRA - RED	3.5% CEM II 32.5 + 3.5 % LIME +1.5 % LIME (ILC)	HMA	3 100 000	·Transverse cracks ·Longitudinal flexural cracks
PALMEIRA - RED	7 % CEM II 32.5+ 1.5 %LIME (ILC)	SEAL	3 500 000	·Longitudinal flexural crack ·Transverse cracks top down
PALMEIRA - RED	5% CEM II 32.5	HMA	1 300 000	·Long and transverse cracking ·Ageing had an important effect
PALMEIRA - RED	2.5 % CEM II 32.5 + 2.5% LIME	HMA	1 400 000	·Longitudinal flexural crack ·Secondary transverse cracking
PALMEIRA - RED	1.5 % CEM II 32.5 + 4.0% SS60	SEAL	200 000*	·Rutting ·Secondary cracking
PALMEIRA - RED	5.5% SS60	SEAL	19 000*	·Rutting ·Seal failed due to debonding and interface distress
DRILLED CORES RECONSTITUTED * Field test	7 % CEM II 32.5	SEAL	125 000	·Longitudinal flexural cracking ·Interface distress

A steeper gradient of stiffness loss is indicative of a more rapid rate of deterioration of the composite pavement. On the other hand a positive increase in the gradient is indicative of a gain in strength. During initial trafficking the 7 percent cement and lime mix exhibited this characteristic. Once it had reached a peak value the loss in stiffness of the 7 percent cement and lime mix was more rapid than the 7 percent cement mix.

Both the lime/cement and pure cement mixes carried 3.1 million axles when testing of both sections was terminated. However at that stage the stiffness ratio of the lime cement at 3.1 million axles was lower than that of the pure cement mix. The expectation was therefore that more severe distress would be found in this section under the same number of load applications. This was indeed found to be the case from diagnostic coring.

The surface seal on the higher strength CTB also performed beyond expectation. Initially the material was kneaded densely until the matrix became totally water tight. There was no evidence of surface shear under the bituminous layer as was found with the low strength treated base courses. It was apparent that the strength at the interface was of paramount importance for increased performance.

The nature of the distress was investigated with a single intrusive exploration through coring. It was found that longitudinal hairline cracking at the bottom of the layer had occurred after 1.3 million load applications. No other distress was evident. The core hole was therefore closed and sealed before trafficking was resumed. Contrarily the nature of distress was very different from that found with the 3 percent CTB mix. Figure 3 show typical distress manifestation in the 3 percent CTB mix.

The good performance of the cemented materials was considered to be due to the high tensile strength of the cemented layers both at the bottom and top of the layers. The extraordinary tenacity of the seal coat section was surprising. It was ascribed to the dense water tightness of the seal once trafficking had kneaded it. The tough surface of the CTB further contributed to the good performance. It was also of importance to realize that the seal coat was left untrafficked for about one month and this maturing period appeared to improve the performance.

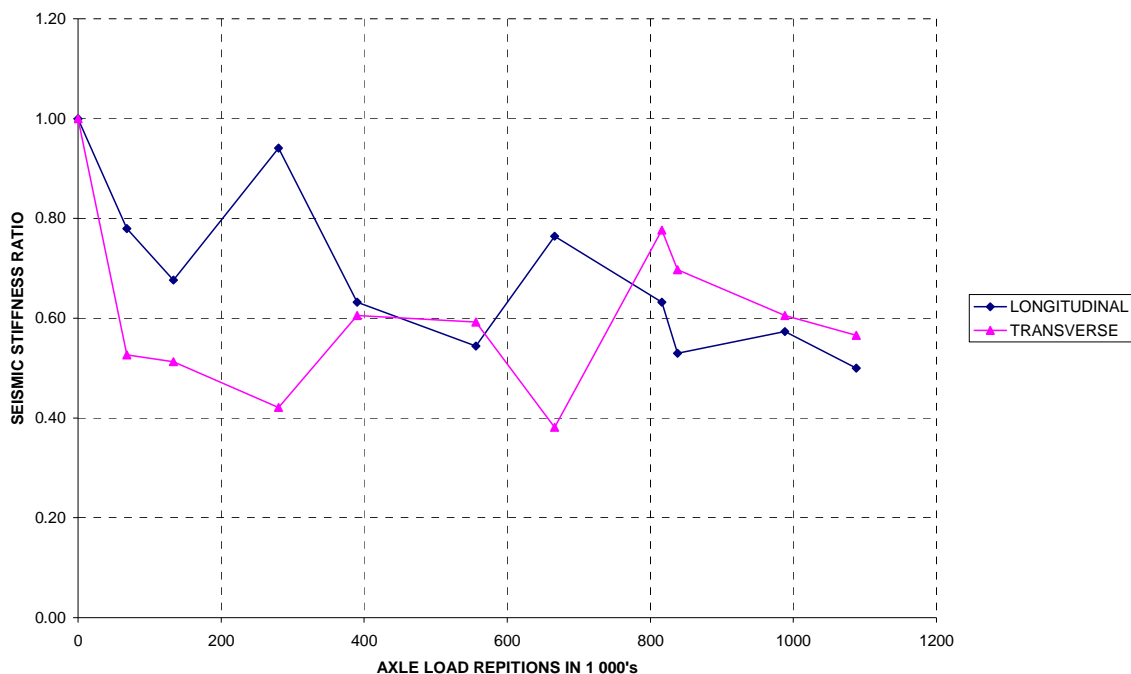


FIGURE 4 Stiffness ratios vs. MMLS3 load applications for 5% cement stabilized red sand base with asphalt surfacing – measured at a point 300 mm from the start of the test section, in longitudinal and transverse relative to traffick direction

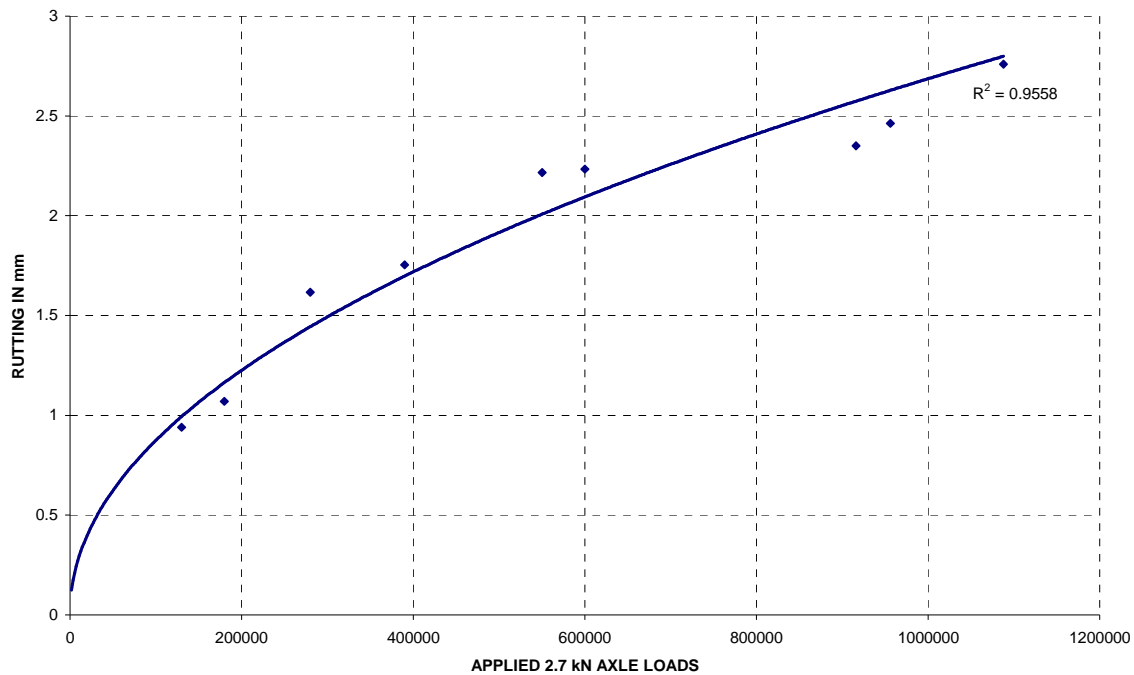


FIGURE 5 Cumulative rut depth with load application for 5 % cement stabilized red sand base with 20 mm asphalt surfacing.

Evaluation of Findings From the MMLS3 Tests

The results from the laboratory MMLS3 tests provide an invaluable source of information for:

1. Comparison of the relative performance of the stabilising agents.
2. Understanding the manifested distress mechanisms
3. Adjudicating the expected pavement performance in order to predict/estimate the full-scale performance characteristics of the test sections

Details are contained in Table 3.

Understanding the Manifested Distress Mechanisms

The distress mechanisms were explored by dissecting the extracted pavement structure and cores. Crack patterns and rupture planes were mapped. By carefully searching for micro-cracks, it was possible to track and discern the crack formation and the manner and sequence in which distress occurred.

- Surface distress under the asphalt surfacing is evident. The distress is aggravated when water ingress occurs during trafficking. Pumping of the CTB material occurs when the CTB surface becomes pulverized at the surface. The pumping appears to be initiated by water infiltrating through cracks in the asphalt. The extent of damage is related to the extent to which water can infiltrate. Relative seismic stiffness ratios (relating the stiffness after trafficking to that before) as low as 0.50 were found where the top of the CTB surface had been pulverized and sand was being pumped out during trafficking.
- Horizontal shear at the interface between the asphalt surfacing and the underlying CTB occurs during trafficking of thin asphaltic surfacing (seal and HMA) when the CTB has a low strength (3 % CTB). This leads to delamination at spots resulting in the erosion of the underlying CTB. The 5% sections appear to be maintaining the bond better
- Longitudinal cracking in the CTB was found in the scaled pavements (and subsequently in the full-scale test pavements) as well as the cores that were tested in the test bed. This phenomenon was also

1
2 observed during the field inspection on old sections of highway EN1, where such cracks had migrated
3 to the pavement surface.

- 4 • The PSPA was successful in monitoring degradation of the pavement structure. It yielded stiffness
5 results in terms of the ratio between trafficked and untrafficked response that reflected the state of the
6 in-situ pavement. As distress and failure increased the ratio progressively reduced. Cores were taken
7 using dry ice for cooling instead of water to help in the determination of the in-situ moisture content.
8 The worst damage appeared in the locations with the highest in-situ moisture content, evidence of the
9 major impact of water ingress.
- 10 • Surface rutting appeared to be related to densification of the asphalt and pulverizing of the top surface
11 of the CTB. No densification of the sand subbase/subgrade was evident.

12 In summary manifestation of distress consisted of the follow:

- 13 1. Bottom up longitudinal cracking
- 14 2. Transverse cracking
- 15 3. Horizontal shear plane forming on the neutral axis of the cement treated base
- 16 4. CTB-HMA interface distress

17 The order and direction of development was dependent on structural composition, material
18 properties and construction history. Some typical failure mechanisms are depicted in the photos in Figures 2 and
19 3.

20 **CONSTRUCTION OF FULL-SCALE FIELD TEST SECTIONS**

21 The specifications for the test sections that were to be built for APT testing were
22 established from the results of the scaled laboratory MML3 performance and issued for construction. Related
23 sampling and testing requirements were also proposed. The construction of test sections was executed according
24 to prescribed guidelines. This was to follow current construction methodology and varying compaction of the
25 cement treated base material with respect to roller type and number of passes. Figure 6 depicts the location of
26 the respective test sections in the test arena. This newly constructed sections are adjacent to the existing
27 rehabilitated road, highway EN1, and are to be utilized as bus stops after testing is complete. Base thickness of
28 all test sections are 150 mm and were constructed on the same subgrade material. Surface type and thickness
29 vary and details are set out in Table 4 and indicated in Figure 6.

30 The results of the respective laboratory tests for material characterization of the respective test sections
31 are shown in Table 4, The sections were cured as prescribed. Construction was completed in June 2005.
32
33
34
35
36
37
38
39
40
41
42
43
44
45
46
47
48
49
50
51
52

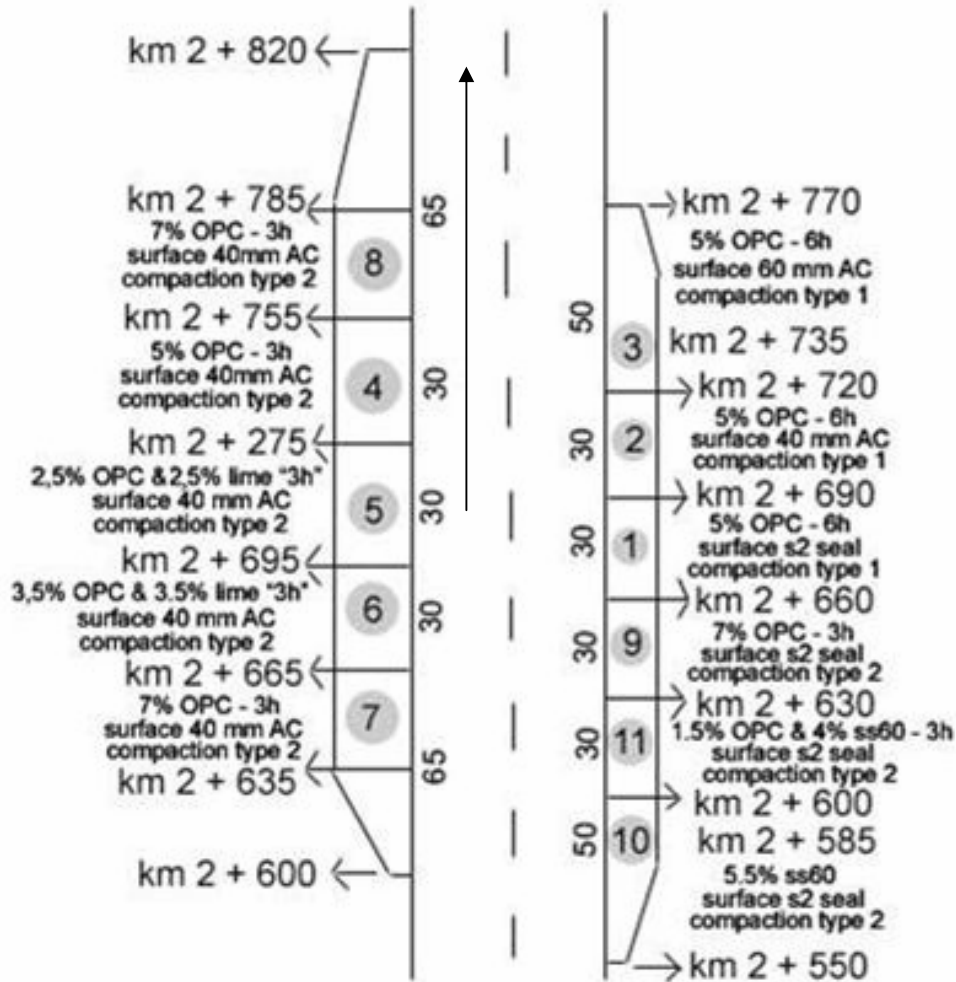


FIGURE 6 Plan view of Test Sections constructed in June 2005

52
51
50
49
48
47
46
45
44
43
42
41
40
39
38
37
36
35
34
33
32
31
30
29
28
27
26
25
24
23
22
21
20
19
18
17
16
15
14
13
12
11
10
9
8
7
6
5
4
3
2
1

Eben De Vos; Fred Hugo ; Pieter Strauss
Jorge Prozzi; Kenneth Fults; Hilario Tayob

TABLE 4 Control test results for Constructed Full-Scale MLS Test Sections

Section No.	1	2	3	4	5	6	7	8	9	10	11
Surfacing	Double Seal	40mm AC	60mm AC	40mm AC	40mm AC	40mm AC	40mm AC	40mm AC	Double Seal	Double Seal	Double Seal
Stabilized with	5% CEMII 32.5			5% CEMII 32.5	2.5% CEMII 32.5 + 2.5% LIME	3.5% CEMII 32.5 + 3.5% LIME	7% CEMII 32.5	7% CEMII 32.5	7% CEMII 32.5	5.5% SS60	1.5% CEMII 32.5 + 4.0% SS60
MATERIAL SOURCE	Palmeira - Red			Palmeira -Red	Palmeira -Red	Palmeira -Yellow	Palmeira -Yellow	Palmeira -Red	Palmeira -Red	Palmeira-Red	Paleira-Red
SIEVE ANALYSIS											
19.0mm				100				100		100	
13.2mm				98	100	100		96	100	98	100
4.75mm	100			94	99	98	100	96	99	98	96
2.0mm	94			85	96	95	96	92	98	97	92
0.425mm	81			79	84	83	44	79	92	81	83
0.075mm	7			15	11	16	6	6	19	15	16
CONSTANTS											
GM	1.81			1.21	1.09	1.06	1.54	1.23	0.91	1.07	1.09
PI	NP			NP	NP	NP	NP	NP	NP	NP	NP
LINEAR SHRINKAGE	0.0			0.0	0.0	0.0	0.0	0.0	0.0	0.0	0.0
MOD AASHTO											
MDD	1956			2025	2012	1887	2022	2023	1948	2069	1951
OMC	10.4			9.0	9.8	10.8	8.4	9.1	9.7	7.8	9.8
MOULDING MOISTURE(%)	10.4			8.7	9.8	11.3	8.2	9.1	9.8	8	11.8
RELATIVE COMPACTION (% of MDD)	97.6			94.1	94.6	102.1	96.7	94.8	96.8	95.4	101.0
ITS											
ITS (KPa)	280.00			600.00	550.00	620.00	300.00	610.00	490.00	280.00	80.00
Avg. Compaction	100.3			99.6	100.2	99.1	98.7	98.6	99.7	97.8	99.1
UCS											
P R O C	COMPACTION %	88.8		89.0	89.2	89.3	89.7	88.7	86.8	91.1	89.8
	UCS(MPa)	0.55		1.56	1.22	1.27	1.05	1.05	0.66	0.43	0.74
M O D	COMPACTION %	98.8		99.7	100.3	98.2	98.8	98.4	99.5	98.1	99.0
	UCS(MPa)	2.42		2.33	3.94	2.38	1.90	3.81	3.53	1.45	0.84

1
2 The APT program was planned to use a research test matrix that contains sections that set the scene for the full
3 spectrum of performance results whether or not they are used in the initial project to which this paper relates.
4 The intent was to explore extreme limits both in terms of poor performance and well-defined good performance.
5 Once this had been achieved, the design guidelines could be established through a process of modelling and
6 interpolation between the MLS 10 and MMLS3 results obtained from the test sections.

7
8 Unfortunately the road users took the sections to be convenient stopping areas for pick-ups and more
9 importantly for repairing break-downs such as gearboxes and axles. This left scars on some of the test sections.
10 The selection of the appropriate areas for the tests therefore had to take this into account. Nevertheless the
11 sections were in general found to be in an acceptable condition when the MLS10 arrived on site for the APT to
12 start in April 2006.

13 **FULL-SCALE AND SCALED FIELD APT BY MEANS OF MLS10 AND MMLS3**

14
15 In order to plan the full-scale trafficking of the test sections of the MLS10, the performance of the respective
16 MMLS3 test sections was taken as a point of departure. The maximum tensile stress at the scaled pavement at
17 the underside of the CTB was calculated. In similar vein the maximum tensile stress of the CTB under the full-
18 scale pavement and wheel loading was calculated. The expected full-scale trafficking yielding similar distress
19 was then calculated on the basis of the “fourth power law” of 4.2. In this analysis it was assumed that material
20 characteristics and test conditions were similar. For example, in the case of the 5% CTB the MMLS3 trafficking
21 was terminated at 1.3 million load applications. The expected full-scale performance was found to be 100 000
22 using 60kN load applications. For the 7 percent CTB the expected full-scale performance yielded 230 000 60
23 kN load applications

24 Accordingly it was concluded that an upper level of 1 million 60 kN load applications would be sufficient to
25 obtain adequate distress for realistic diagnostic analyses.

26 Full-scale test load characteristics are set out in Table 1. Environmental conditioning of the full scale tests were
27 cyclic ambient dry and wet pavement surface conditions similar to the scaled APT. Trafficking was alternated
28 between 200 000 ambient dry and 50 000 load cycles with water sprayed onto the pavement surface.

29 The sequence of testing with the MLS10 was determined with due regard to the findings of the laboratory
30 MMLS3 tests. Accordingly, the 5 percent CTB structures were selected for the first MLS10 tests namely
31 sections 4 and 5. This was to be followed by sections 1 and 7 where the binder content had been increased to 7
32 percent. Thus far three tests have been completed.

33 In view of the findings discussed below it was decided to limit load applications on each of the respective
34 sections to a level perceived to provide the most information towards the understanding of differences in
35 performance and response. Monitoring entailed the following:

- 36 • PSPA measurements
- 37 • Dynamic Surface Deflections
- 38 • Surface deformation
- 39 • Crack manifestation

40
41 The results have been very informative. Details are discussed below. The details pertaining to the load
42 applications of the full-scale sections are shown in Table 5. The discrepancy between the expected and actual
43 performance could be ascribed to the extent of aging before initiation of trafficking. Full-scale sections aged
44 ten months before trafficking commenced whereas scaled tests aged between two weeks and one month.
45
46
47
48
49
50
51
52

TABLE 5 Summary of MLS10 Tests to Date

SECTION	8*	4	5a	5b
Stabilizing Binder	7 % CEM	5 % CEM	2.5% C 2.5% L	2.5% C 2.5% L
Sand (150mm)	RED	RED	RED	RED
Surfacing (40mm)	HMA	HMA	HMA	HMA
Axle load applications (60kN)	84500	330000	100000	1080000

Pavement behaviour at different stages of distress during trafficking were observed to be similar for the tested sections, but they occurred at different load applications. The pavement surfaces started to roll dynamically in wave form under loading tyres, with deflections visible with the naked eye.

Stiffness response during trafficking in terms of PSPA measurements

The stiffness of upper 200 mm of the pavement structure was measured at regular intervals during trafficking by means of the PSPA. Typical seismic modulus plots for a specific position in the test section relative to the wheel path are shown in Figure 7a. The change in stiffness is clearly evident as the trafficking increased. PSPA measurements were taken at five locations relative to the wheel configuration, at three different points along the test section.

The findings were as expected namely a reduction due to the distress under the trafficking. More important was the nature of the change in the stiffness. In general the change in longitudinal stiffness was more than that in the transverse direction. This was probably to a large extent due to the faster growth in the cracks in the transverse direction than the cracks in the longitudinal direction. Figure 7 b, d illustrate the relative decrease in stiffness for specific points under the loading wheel, where Figure 7c illustrates the trends in stiffness performance with load application.

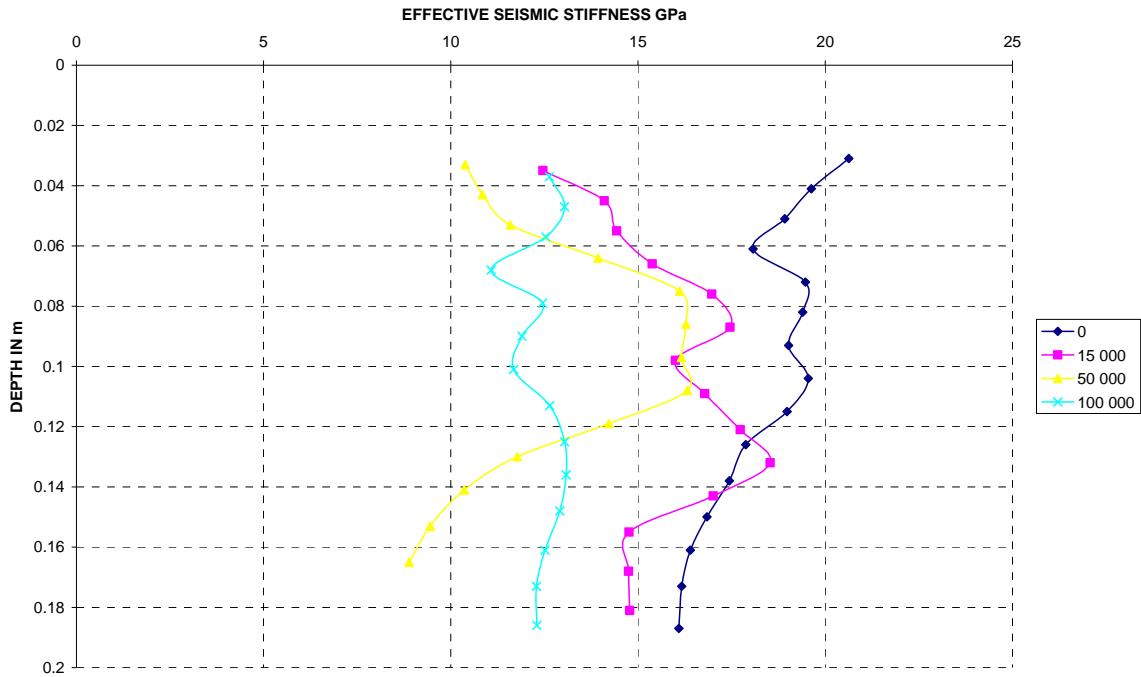


FIGURE 7a Typical Seismic Stiffness Profiles with Axle Load Application at a specific point relative to the wheel track

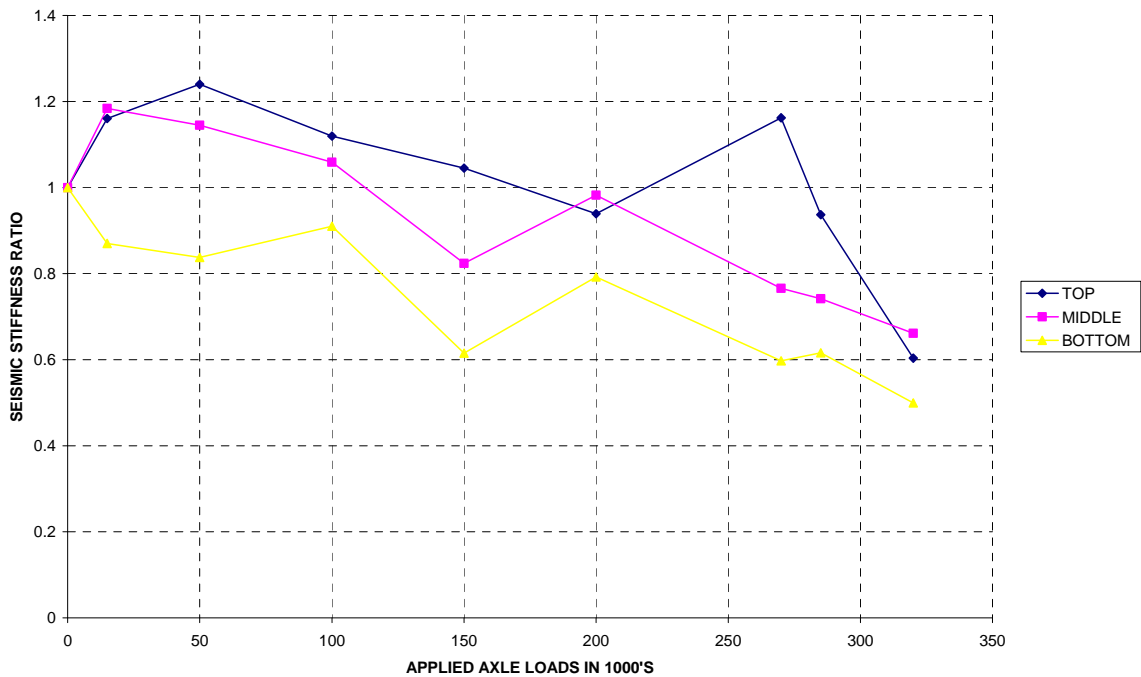


FIGURE 7b Seismic Stiffness Ratios vs. Load Application for Section 4, Position 2 in the Left Wheel track, Longitudinal Direction

1
2
3
4
5
6
7
8
9
10
11
12
13
14
15
16
17
18
19
20
21
22
23
24
25
26
27
28
29
30
31
32
33
34
35
36
37
38
39
40
41
42
43
44
45
46
47
48
49
50
51
52

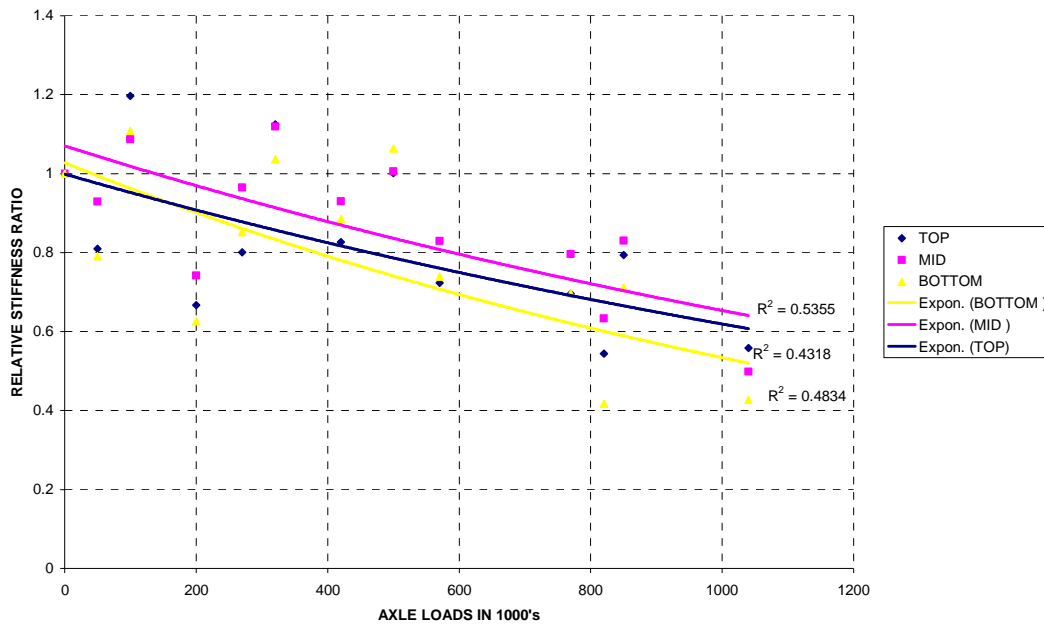


FIGURE 7c Trends in stiffness reduction for Section 5b Position 2 in the Left Wheel track, Longitudinal to the direction of traffic

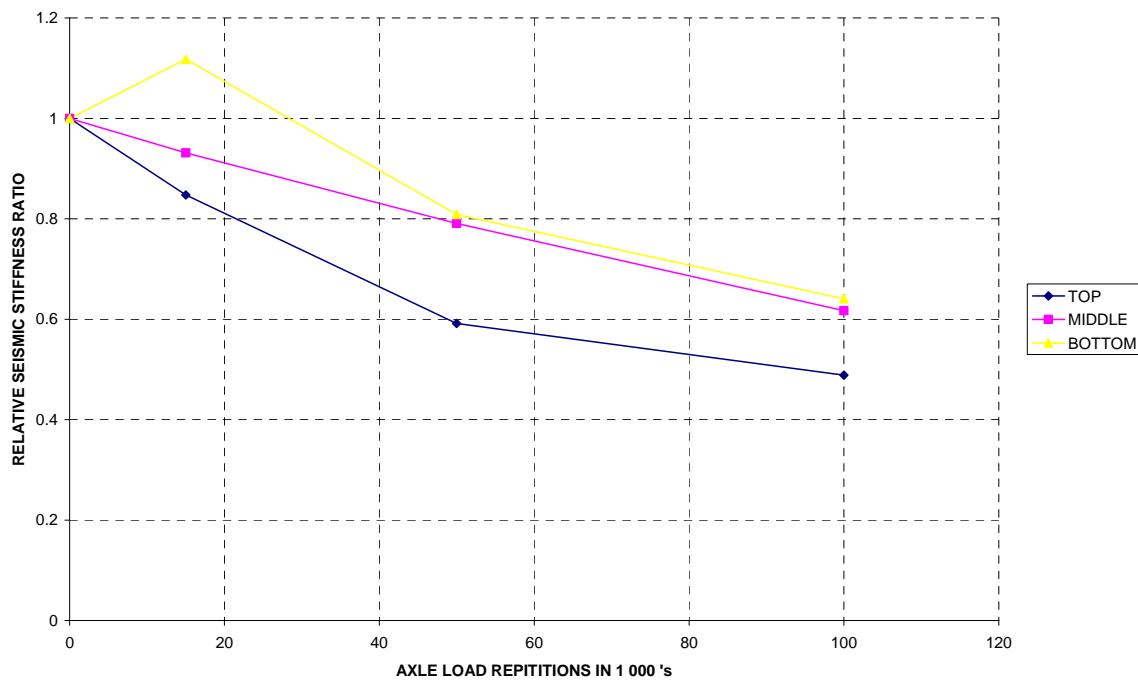


FIGURE 7d Relative Seismic Stiffness Ratio vs. Axle Load Repetitions for Section 5A Left Wheel Track Measured in Transverse Direction

1
2
3
4
5
6
7
8
9
10
11
12
13
14
15
16
17
18
19
20
21
22
23
24
25
26
27
28
29
30
31
32
33
34
35
36
37
38
39
40
41
42
43
44
45
46
47
48
49
50
51
52

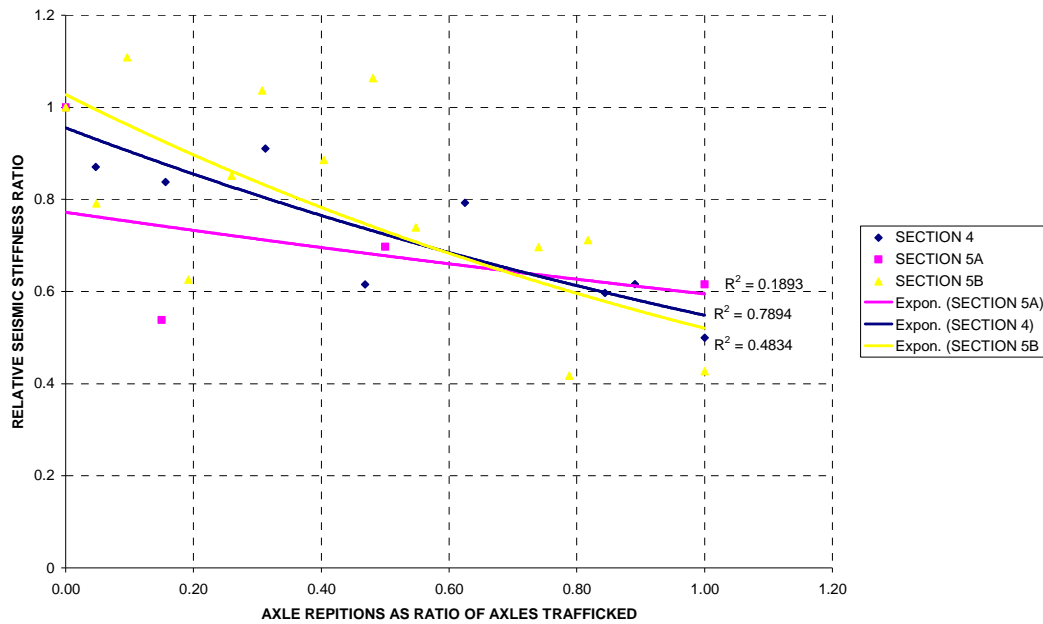


FIGURE 7e Relative Seismic Stiffness Ratio vs. Trafficked Axle Ratio for Test Sections 4, 5A and 5B, depicting relative trends in performance.

Dynamic Deflection Profiles

Dynamic Deflection profiles were monitored intermittently during trafficking by means of a Modified Benkelman Beam instrumented with a LVDT. Measurements were taken at different speeds on the same spot namely 120mm in front of the centre of the test section. It is apparent that the deflections increased as the speed was increased. The reason for this increase was not readily apparent but the response was similar for all tests.

As the pavement suffered distress the deflections progressively increased. See Figure 8a. When the trafficking was terminated the deflections had in general doubled relative to the initial deflections. This response was just the opposite of the stiffness ratios that were discussed earlier. The two parameters were inversely proportionate to each other.

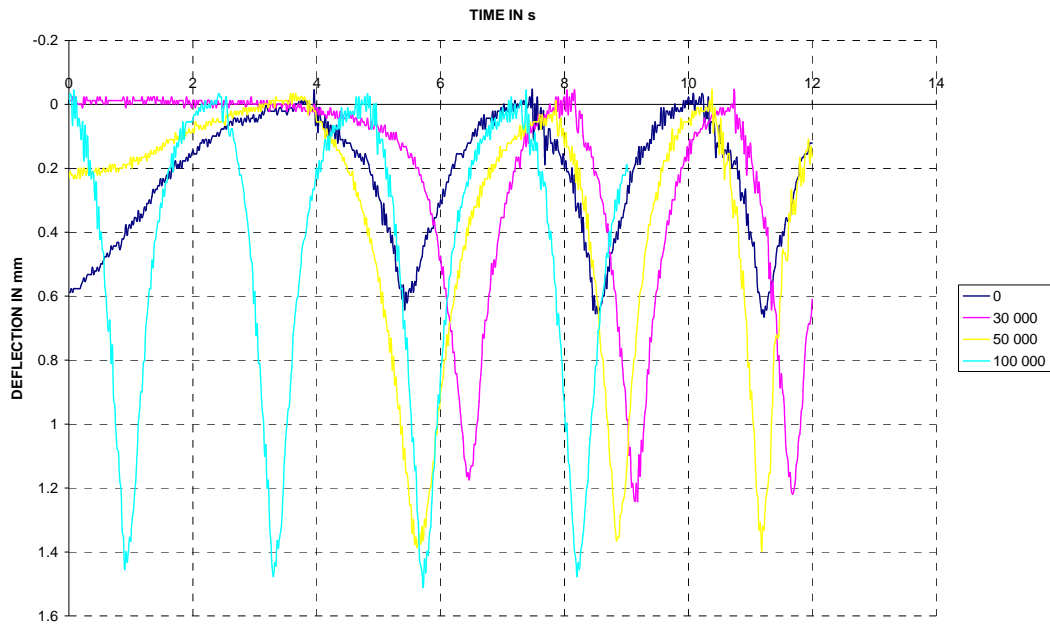


FIGURE 8a Deflection profiles for section 5a monitored at intervals during axle load trafficking

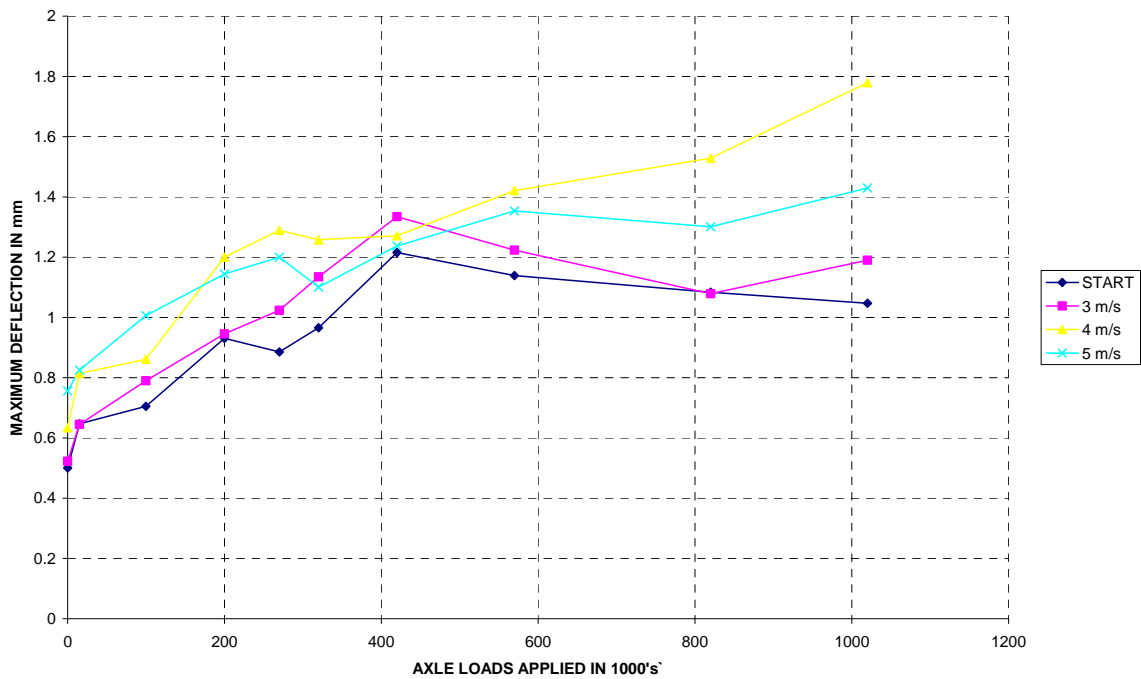


FIGURE 8b Maximum Deflection at Slow Speed for Section 5B vs. Axle Load Application

Rutting Due to Trafficking

Rutting was monitored intermittently during trafficking by an electronic profilometer accurate to 0.1mm. Typical results are shown in Figure 9a and the cumulative effect is depicted in Figure 9b. In contrast to HMA

1
2
3
4
5
6
7
8
9
10
11
12
13
14
15
16
17
18
19
20
21
22
23
24
25
26
27
28
29
30
31
32
33
34
35
36
37
38
39
40
41
42
43
44
45
46
47
48
49
50
51
52

pavements, the initial increase in rutting of the composite CTB HMA pavement was more gradual. From a comparison of Figure 5 and 9b it is apparent that the rutting performance of the scaled and full-scale pavements was similar.

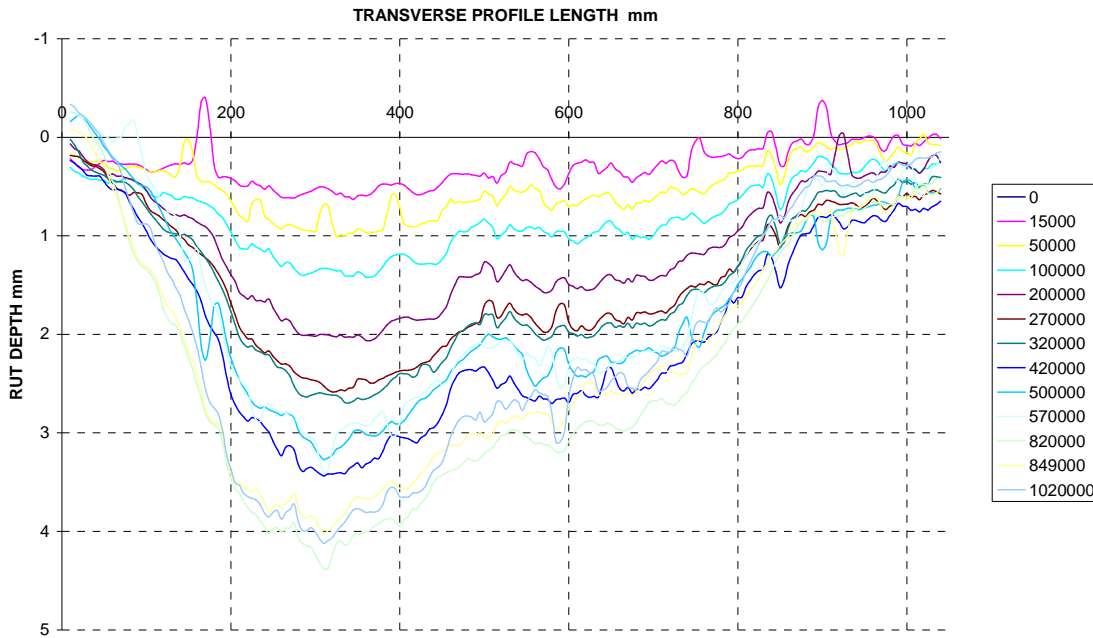


FIGURE 9a Transverse rutting profiles with load applications for the center of MLS10 Test section 5

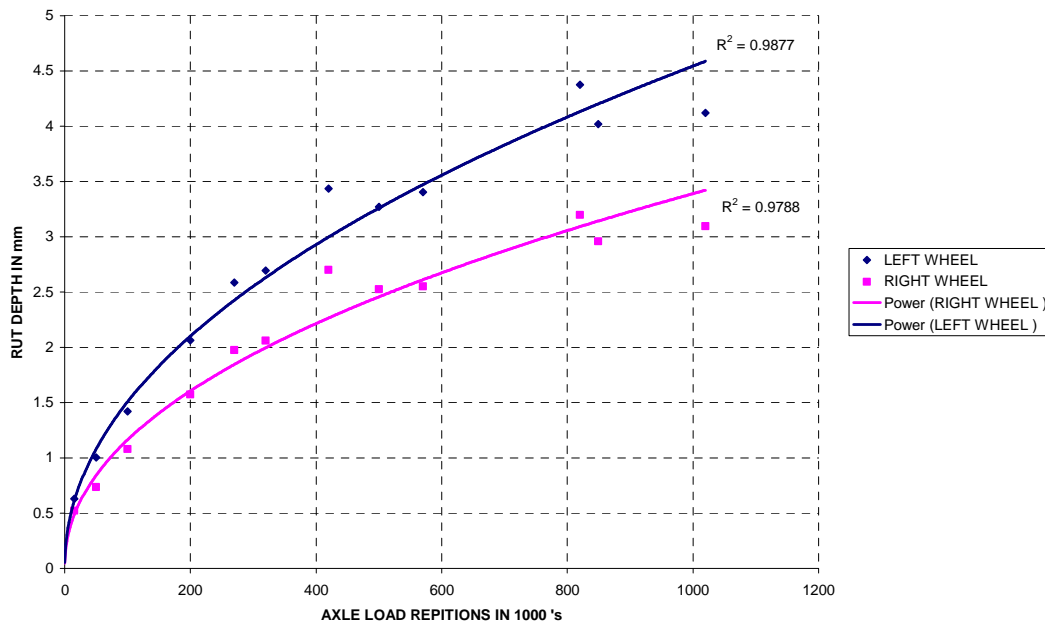


FIGURE 9b Cumulative maximum rut depth at the middle of MLS10 test section 5 - left and right wheel path

1
2
3
4
5
6
7
8
9
10
11
12
13
14
15
16
17
18
19
20
21
22
23
24
25
26
27
28
29
30
31
32
33
34
35
36
37
38
39
40
41
42
43
44
45
46
47
48
49
50
51
52

Diagnostic evaluation

A trench was excavated across the wheel path of section 4 to explore the nature of distress. Figure 10a and 10b show the extracted block structure reconstituted to reflect the geomorphology. The underside of the asphalt surfacing with marked cracks is shown in Figure 10c. The similarity of the distress between the full-scale and the laboratory scaled pavements is apparent from the MMLS3 diagnostic specimens shown in Figures 3a and 3b.

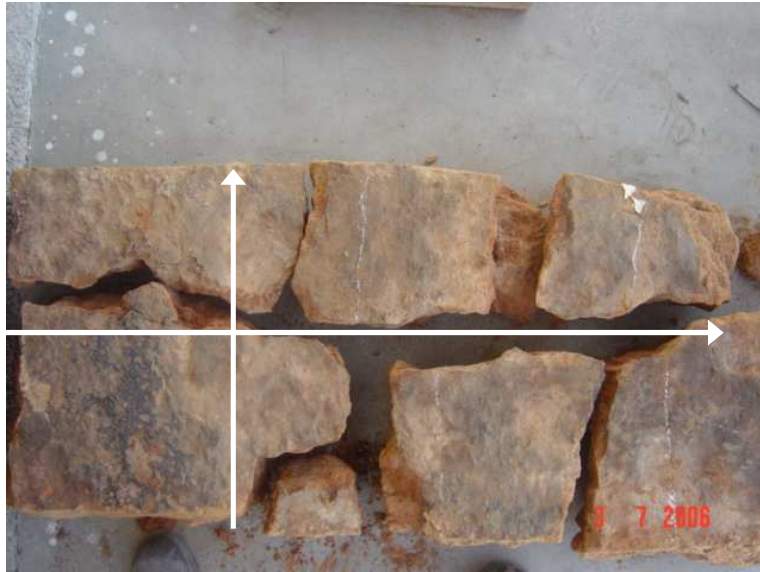


FIGURE 10a Plan View of the CTB slab extracted from full scale test section 4 for diagnostic investigation (550x1200)



FIGURE 10b Elevation View of the CTB slab extracted from full-scale test section 4 for diagnostic investigation (160x1200)



FIGURE 10c View of underside of HMA extracted from full scale test section 4 for diagnostic investigation showing marked positions of cracks.

Interim Test Findings

Although the study is not yet complete, some important findings have already emerged albeit from the current small base of research.

1. Use of the MMLS3 for testing scaled sand CTB pavement layers was found feasible and the results compatible with those developed under full-scale MLS10 testing. This new application of the system ratifies research by Kim et al, (1998) on scaled applications of APT. This rendered parallel application of MMLS3 and MLS10 APT an effective way of broadening the scope of the study.
2. A significant feature has been the similarity between laboratory and field performance of the pavements in terms of distress and number of axle load applications. This lends support for the decision to use MMLS3 testing to scope the study as an efficient and effective way of developing the research program. Detailed analysis of the trafficking performance is beyond the scope of the paper.
3. Use of seismic wave propagation for monitoring stiffness changes due to trafficking under APT was successful. The system detected increased distress in the pavement layers before manifestation on the surface. With careful application, it was possible to discern the nature of the distress. This lends further support for the use of a device such as the P SPA as a non-destructive accessory tool with APT.
4. The distress mechanisms identified in the pavement system during the study were excellent replicas of those found in similar pavement structures in the region. The data will provide the basis for modelling the performance of the CTB pavement structures appropriate for use in the region. This should serve to support the preservation and maintenance efforts that are underway in Mozambique.
5. The different distress modes causing disintegration of the structure were found to occur in different sequences depending on the structure of the pavement and the strength of the materials.
6. The application of wet trafficking intermittently with dry trafficking was found to be feasible. It provided a means of ensuring that micro damage to the pavement is subjected to the effect of pore pressure under the impact of tyres. Further research will be needed to quantify such impact.
7. With the pavements investigated in this study, two noteworthy response relationships were found.
 - a. On average, dynamic deflection progressively increased relative to initial value, trending towards two at failure - Figure 9b.
 - b. Concurrently PSPA stiffness's decrease progressively, with the stiffness ratio reaching 50 percent of initial value when significant distress has manifested – Figure 8d.

These relationships will be explored further in the remainder of the study to establish general applicability.

1
2 **CONCLUSION**

3 Application of APT as a research tool in the quest for developing guidelines for a
4 mechanistic-empirical pavement design method for cement stabilized coastal sand bases in Mozambique is
5 proving to be both effective and efficient.
6

7 **ACKNOWLEDGEMENTS**

8 The research that was reported in this paper was done as an integral part of project ,
9 206/CON/ES/DEN/2003 for the ANE. The funding was sponsored by the World Bank. The authors gratefully
10 acknowledge permission to publish the findings. The opinions expressed by the authors in the paper do not
11 necessarily reflect those of these organizations.
12
13
14
15
16
17
18
19
20
21
22
23
24
25
26
27
28
29
30
31
32
33
34
35
36
37
38
39
40
41
42
43
44
45
46
47
48
49
50
51
52

1
2
3
4
5
6
7
8
9
10
11
12
13
14
15
16
17
18
19
20
21
22
23
24
25
26
27
28
29
30
31
32
33
34
35
36
37
38
39
40
41
42
43
44
45
46
47
48
49
50
51
52

REFERENCES

- (1) Strauss Pieter, Hugo Fred, Slavik Martin, de Vos Eben R, Fults Kenneth, Smit Andre de Fortier, Prozzi Jorge A, 2005 Interim report under Contract 206/CON/ES/DEN/2003: The Evaluation of Long Term Behaviour of Pavement Layered Materials by Means of Accelerated Pavement and Supplementation/Verification Testing in Mozambique. Texas August 31.
- (2) Kim S.M., Hugo F. and Roeset J.M. 1998. Small-Scale Accelerated Pavement Testing, Journal of Transportation Engineering, ASCE, Vol. 124, No.2, Mar/Apr 1998, pp. 117-122.
- (3) Nazarian S, Tandon V, Yuan D. 2002, Mechanistic Quality Management of Asphalt Concrete Layers with Seismic Methods, Journal of Testing and Evaluation, Sept.
- (4) Nazarian, S., Baker, M. and Crain, K., "Assessing Quality of Concrete with Wave Propagation Techniques," *Materials Journal, American Concrete Institute*, Vol. 94, No. 4, 1997, pp. 296-306.
- (5) Hugo, Fred, Smit Andre de Fortier, Poolman Pieter, Powell Buzz, Bacchi Chris, 2004 Distress of hot mix asphalt on the NCAT test track due to accelerated wet trafficking with the MMLS3, CD-ROM Proceedings Second International APT Conference, Minneapolis, USA.
- (6) Lee Sugjoon and Kim Y. Richard 2004, Development of Fatigue Cracking Test Protocol and Life Prediction Methodology Using MMLS3 Proceedings Fifth International RILEM Conference on Cracking, Limoges, France, May